General Disclaimer

One or more of the Following Statements may affect this Document

- This document has been reproduced from the best copy furnished by the organizational source. It is being released in the interest of making available as much information as possible.

- This document may contain data, which exceeds the sheet parameters. It was furnished in this condition by the organizational source and is the best copy available.

- This document may contain tone-on-tone or color graphs, charts and/or pictures, which have been reproduced in black and white.

- This document is paginated as submitted by the original source.

- Portions of this document are not fully legible due to the historical nature of some of the material. However, it is the best reproduction available from the original submission.

Produced by the NASA Center for Aerospace Information (CASI)

Lockheed

MISSILES & SPACE COMPANY

A GROUP DIVISION OF LOCKHEED AIRCRAFT CORPORATION

SUNNYVALE, CALIFORNIA

LOCKHEED MISSILES & SPACE COMPANY

HUNTSVILLE RESEARCH & ENGINEERING CENTER

HUNTSVILLE RESEARCH PARK

4800 BRADFORD BLVD., HUNTSVILLE, ALABAMA

CONTROL SYSTEM OPTIMIZATION
FOR SATURN V LAUNCH VEHICLES
USING GRADIENT TECHNIQUES

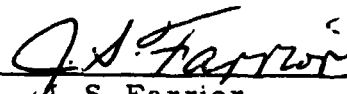## FINAL REPORT

February 1970

Contract NAS8-30515

by

C. L. Connor
W. Trautwein

APPROVED BY: _____

T. R. Beal, Manager
Dynamics & Guidance Dept.

_____
J. S. Farrior
Resident Director

FOREWORD

This document represents work performed by Lockheed's Huntsville Research & Engineering Center for NASA-Marshall Space Flight Center under Contract NAS8-30515, Modification 2, Task 1. It describes the results of an application study where a new computerized method for optimal control system design was applied to the Saturn V load relief program. Together with LMSC/HREC D162122-II and LMSC/HREC D162122-III, these constitute the final reports under this contract. The report, LMSC/HREC D162122-III, represents a User's Manual to be used as an aid in applying this hybrid optimization technique to other control system design problems.

CONTENTS

Section 1

INTRODUCTION AND SUMMARY

This study is a continuation of previous work to develop a computerized method for the engineering design of attitude control systems. For a specified form of the control law as dictated by available sensors and limitations in cost and complexity, the design procedure leads to time-varying control gain schedules which minimize a given performance criterion. The variational problem of finding optimal time-varying controller parameters (gains) is reduced to a sequence of parameter searches which result in near-optimal piecewise linear gain schedules and are rapidly determined by an efficient hybrid computing scheme.

Hybrid computation is applied to enable both realistic simulation of vehicle dynamics on the analog console and iterative adjustments of critical controller parameters based on optimum-seeking modern gradient techniques in the digital unit. The approach thus combines the practical features of analog simulation with the systematic parameter search methods of multi-dimensional gradient techniques.

A practical feature of the method is the possibility to specify design goals in the most direct manner with virtually no mathematical constraints concerning its functional form.

As an application example, the Saturn V attitude control problem was chosen. The specific design goal was to find controller adjustments which would minimize peak bending loads due to representative wind forces and due to an engine failure at a critical flight time.

The high degree of flexibility in selecting performance criteria of arbitrary form was fully utilized by choosing a minimax criterion. It was

Wind Disturbance α_w $8°$

Failure Mode Engine No. 1 $\begin{cases} \text{Out} \\ \text{In} \end{cases}$

Leeward Engine Failure

a_o

Optimized Gain Schedules $\begin{cases} a_1 \\ (\text{sec}) \\ a_2 \left(\dfrac{\text{deg}}{\text{m/sec}^2}\right) \end{cases}$

1 0

4 0

Pitch Angle ϕ (deg) 4 0

Engine Deflection β (deg) $+5.0$ 0

Bending Moments at Station 3764 $\dfrac{M_{B3}}{\overline{M}_{B3}}$ $+.5$ 0

Peak Moment for Constant Gain Case 53% higher than peaks of optimized system

At Station 1541 $\dfrac{M_{B1}}{\overline{M}_{B1}}$ $+.5$ 0

Peak Moment for Constant Gain Case 50% higher than peaks of optimized system

Flight Time - sec

60 70 80 90

Fig. 1-1 - Typical Saturn V S-IC Optimization Results from Previous Study Phase. Three Gain Schedules are Optimally Adjusted to Minimize the Peak Bending Loads Among Two Stations (1541 and 3764) for the Disturbance and Failure History of the Top Charts. Peak Loads are Substantially Reduced Compared with Nominal Saturn V Performance (without Accelerometer Feedback). The Wind Disturbance used is the MSFC 95% Synthetic Wind Profile with Superimposed Gust at Maximum qα with Maximum May-December Envelope. (Refs. 4 through 7.)

found to be the most selective and most direct mathematical representation
of the design goal. The absolute value of the peak bending load at the worst
of several stations along the vehicle was used as the major term in the per-
formance index to be minimized during optimization.

1.1   RESULTS FROM PREVIOUS STUDY

The program was successful in solving this difficult "minimax" prob-
lem of minimizing the maximum of several functions. In previous applica-
tion studies, it was assumed that an engine failure occurs at a critical flight
time when the vehicle is subjected to severe wind disturbances. A typical
result is shown in Fig. 1-1. For specific disturbance and failure histories
as recorded in the upper strips, peak loads are substantially reduced as
compared with nominal Saturn V performance as seen in the bottom strips.
These reductions are due to an additional accelerometer feedback channel
and optimal time-varying adjustments of the three feedback gains. The opti-
mized piecewise linear gain schedules recorded in strips 3 through 5 start
from the nominal Saturn V adjustments at time 60 sec. A subsequent reduc-
tion of the attitude gain a_o and increasing accelerometer gain g_2 reduces
bending load peaks caused by the assumed engine failure. The minimax per-
formance criterion used is illustrated in Fig. 1-2. It reflects the load relief
objective better than any of the standard forms. The observed bending loads
M_{B1}, M_{B2}, M_{B3} were normalized with respect to the structural limits at the
three critical stations. The only freely adjustable weighting factor q was
readily selected during a few trial optimizations so that trajectory deviations
remained within acceptable levels. Thus, a major shortcoming of linear con-
trol theory, the difficulty to relate a large number of necessary weighting
factors to the physical design goal, was virtually eliminated.

The assumed engine failure introduces severe disturbance torques
which are about five times stronger than the assumed wind loads. It must
therefore be expected that such factors as the location of the assumed failing
engine would have a major effect on the optimization. As a result, the optimal
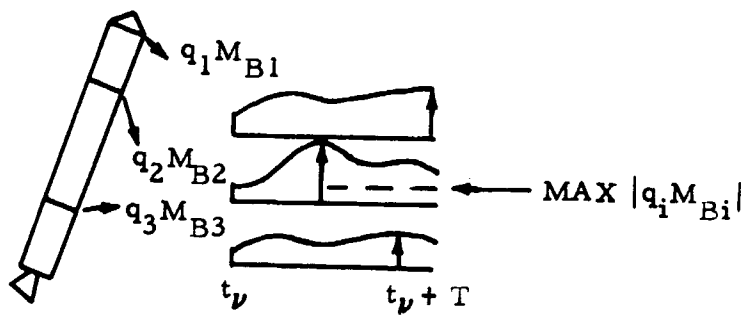
Fig. 1 - 2: Load Relief Performance Criterion Used in Previous Studies:

$$J = MAX \ |q_i M_{Bi}(t)| + q \int_{t_\nu}^{t_\nu + T} \theta_{RG}^2 (t) \ dt \longrightarrow MIN$$

$$i = 1, \ 2, \ 3 \qquad$$

$$t_\nu \leq t < T$$

$\underbrace{\qquad\qquad}$

Normalized
Peak Bending
Loads

$\underbrace{\qquad\qquad}$

Mean Square of
Rate Gyro Output to
Ensure Trajectory
Stability

gain schedules based upon an assumed failure of a leeward engine differ substantially from the schedules optimally adjusted for a windward engine failure. This sensitivity to unpredictable events, a common problem in all time-domain design methods, severely limited the application of the technique in its previous state of development.

1.2   MAJOR RESULTS OF PRESENT STUDY

One further step was necessary in order to bring the hybrid optimization scheme to the point of usefulness as a true design tool. Previous efforts were concentrated solely on application to the problem of optimizing control system parameters for isolated environmental and failure conditions. In real life, however, a system must be designed to operate successfully under any of a number of such conditions, and the system has no way of "knowing" before the fact which of these conditions will actually be encountered. Thus, a truly optimal system is one which anticipates the occurrence of a number of possible conditions, tests performance against a criterion which is a function of all these possible conditions, and adjusts the control parameters so as to optimize this performance criterion. In the case of the booster load relief problem, one might want to formulate the performance criterion to be the maximum bending moment which would occur within T seconds into the future, assuming the possibility of occurrence of a variety of different environmental or failure conditions.

This important generalization of the optimization method was achieved by extending the performance evaluation process to at least two adverse flight or failure conditions, all of which are simulated repetitively during the optimization process.

In the booster load relief problem where engine failure modes are included, the two most adverse flight conditions were:

    A.   <u>Failure of a Windward Engine</u> near the time of maximum dynamic pressure and peak horizontal wind loads.

or

    B.   <u>Failure of a Leeward Engine</u> near the time of maximum dynamic pressure and peak horizontal wind loads.

As a realistic test case, these two adverse cases were therefore selected for simultaneous consideration in the optimal controller design. The performance criterion chosen is illustrated in Fig. 1-3.

As a result, the optimized controller gain schedules represent the best trade-off considering the possibility of occurrence of any of these flight conditions. Typical results are plotted in Fig. 1-4. Peak bending loads for the two failure cases vary from 28% to 48% of the structural limits $\bar{M}_B$, using constant Saturn V controller gains without accelerometer feedback. The set of time-varying gain schedules obtained through simultaneous optimization for both failure modes leads to almost identical peak loads for both flight conditions and all load stations considered. The worst case loads of Case B are reduced by 31% at the price of an 18% increase in loads for the previously non-critical case A. An ideal compromise is achieved.

The efficiency of the hybrid optimization method was also increased during this study phase. Typical computing speeds make possible 40 simulations per second with varying amounts of digital computation between subsequent simulations.

$q_1 M_{B1}$

$q_2 M_{B2}$

$q_3 M_{B3}$

Flight Condition A
(Windward Engine Out)

$q_1 M_{B1}$

$q_2 M_{B2}$

$q_3 M_{B3}$

Flight Condition B
(Leeward Engine Out)
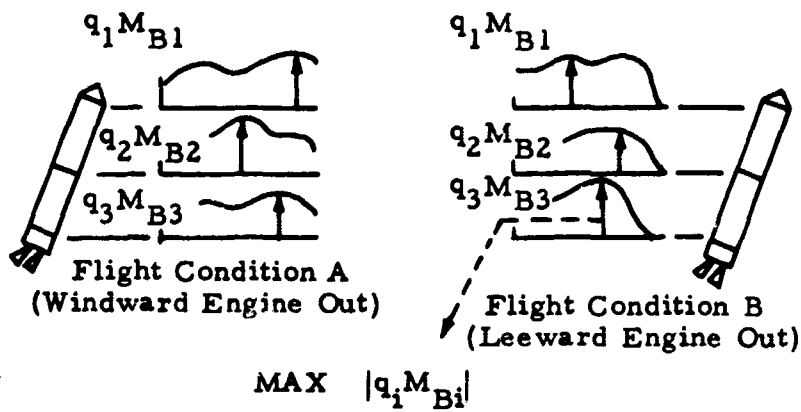
MAX $|q_i M_{Bi}|$

Fig. 1-3 - Generalized Load Relief Performance Criterion Used in Present Studies:

$$J = \text{MAX } |q_i M_{Bi}| + \int_{t_\nu}^{t_\nu + T} \theta^2_{RG}(t)\,dt \longrightarrow \text{MIN}$$

Case A, Case B

$i = 1, 2, 3$

$t_\nu < t < t_\nu + T$

NOTE: Performance Index is a function of two (or more) different flight conditions.
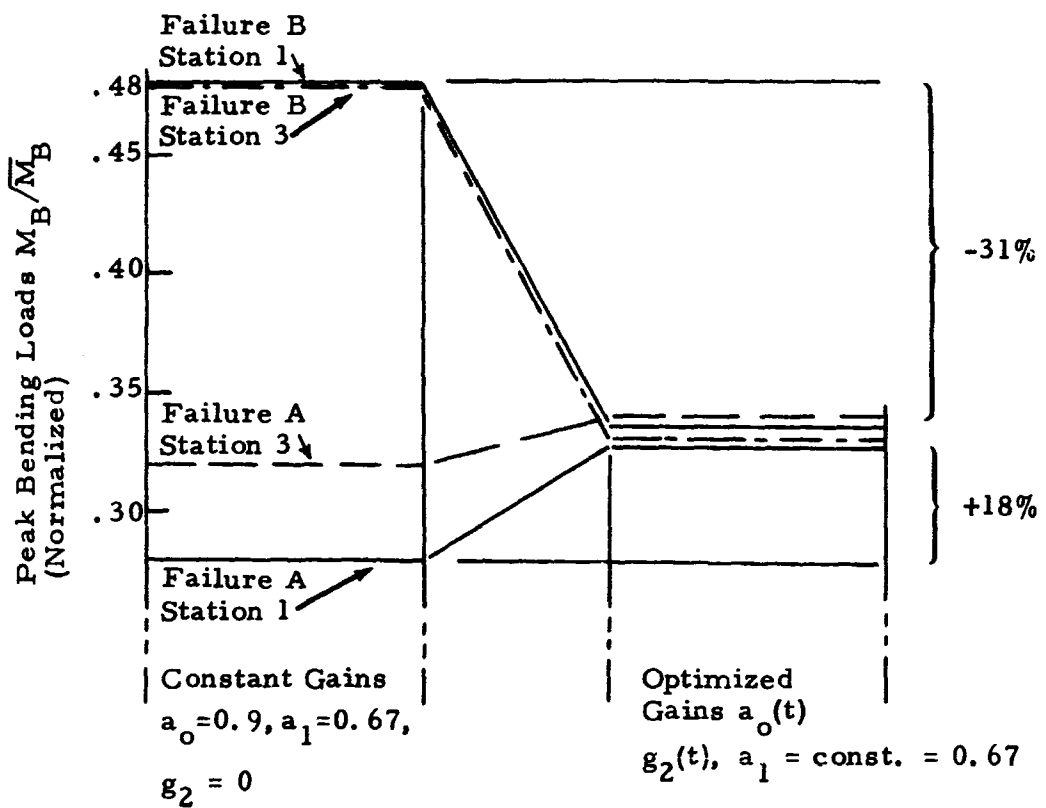
Fig. 1-4 - Peak Bending Loads for Saturn V S-IC Powered Flight
Compared for Constant Gain Case and for Case Optimized
for Failure of Leeward or Windward Engine. Wind Profile
as in Fig 1-1; Assumed Engine Failure Time 83 sec.

Section 2
OPTIMIZATION TECHNIQUE AND RECENT MODIFICATIONS

2.1   GENERAL DESCRIPTION OF OPTIMIZATION SCHEME

The optimization method is a direct method where only forward integrations of the dynamic equations are performed. To this end, the vehicle dynamics and control loops are simulated on the analog console of a hybrid computer as shown schematically in Fig. 2-1. During each simulation, the performance is evaluated by computing the performance index, J. After the simulation, J is transferred to the digital console where a minimization scheme is programmed to determine the minimum of J with respect to the adjustable parameters. During development of the optimization method it was found that with no loss of optimality the optimization can be carried out independently over a number of limited time intervals rather than simultaneously over the entire flight time. The total flight time under study is therefore divided into a finite number of update intervals of length $(t_{\nu+1} - t_{\nu}) = \Delta t$ of typically 5 sec as indicated in Fig. 2-2. Figure 2-3 shows how the linear gain schedules are evaluated at each update interval.

While rigorous optimal gain schedules as obtained from calculus of variations will be general functions of time, the class of optimal gain schedules to be generated by the present method was restricted to piecewise linear functions of time as in Fig. 2-2. This largely reduces the computational load and at the same time keeps the resulting optimal schedules closer to a practical form for implementation. Discontinuous piecewise constant schedules have been found to be unsuitable in this approach because of the transients that result from step-type gain changes.

The problem to be solved by the minimization scheme programmed on the digital console can then be stated as follows: Find a set of gain slopes $\dot{a}_o, \dot{a}_1, \dot{g}_2$, so that the performance index, J, is minimized in the look-ahead

Parameter Changes, Failure Modes and
Wind Inputs (Mean Plus Gusts)

Actuator &
Engine Dynamics
A(s)

Vehicle Dynamics
Including Bending
Sloshing

Rate Gyro

Accelerometer

Attitude
Gyro

Performance Analyzer

$$J = J \left[M_B(x_j) \right]_{t_\nu}^{t_{\nu+T}}$$

$\nu = 1, \ldots r$

ν is No. of Polygonal
Segments of Gain
Schedules

a_o

Filter
$F_\phi(s)$

ϕ_i

g_2

Filter
F_A

a_1

Filter
$F_{\dot\phi}(s)$

$\dot\phi_i$

J

Analog

A/D

a_1

Gain Schedules

$$\int \overline{K}_i dt = \begin{bmatrix} a_o(t) \\ a_1(t) \\ g_2(t) \end{bmatrix}$$

Digital

∫

$\dot{g}_2$

D/A

Gradient Minimization
Scheme (Fletcher-
Powell) see Fig. 2-5

∫

$\dot{a}_o$

D/A

∫

$\dot{a}_1$

D/A

Slope Adjustments $\overline{K}_i = \left[\dot{a}_o, \dot{a}_1, \dot{g}_2 \right]^T$

Figure 2-1 – Mechanization of Optimization Method Based on Finite
Optimization Intervals and on Polygonal Gain Schedules
on Hybrid Computer
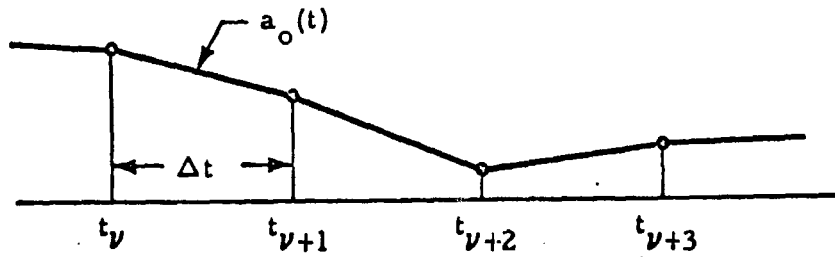
Fig. 2-2:   Desired Polygonal Form of Optimal Gain Schedules.
(Typical Update Interval Δt During Study was 5 sec.)
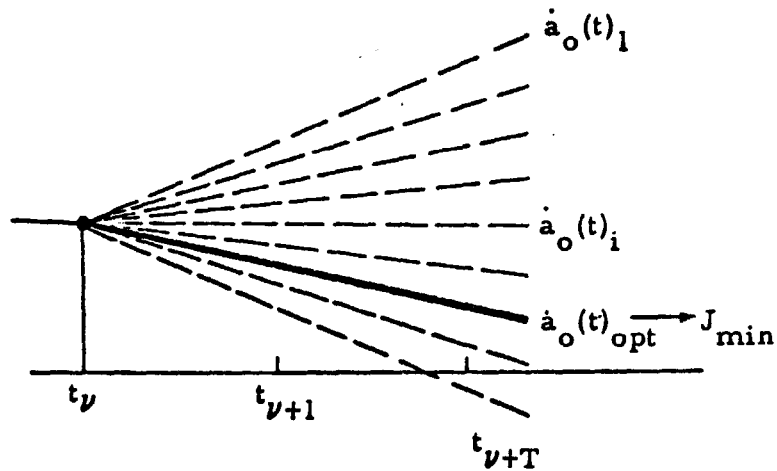
Fig. 2-3 -   During Optimization Cycle at Flight Time t_ν, a Large
Number of Linear Gain Schedules are Evaluated for
their Load Relief Performance. Optimization Interval
(Look-Ahead Interval) T was Varied During Study
Between 10 and 20 sec).

interval under study. J may therefore be written in the functional form

$$J = J(\dot{a}_o, \dot{a}_1, \dot{g}_2) \rightarrow \min$$

The search in the $\dot{a}_o, \dot{a}_1, \dot{g}_2$ parameter space for the optimum is performed in two phases as sketched in Fig. 2-4 for a two-dimensional case assuming one parameter ($\dot{a}_1$) is kept constant:

- Systematic Grid Search

 All possible parameter combinations within a grid of specified limits and fineness are evaluated for J. This complete survey of parameter space largely reduces the risk of finding local rather than absolute minima.

- Gradient Search

  A powerful gradient minimization scheme based on the method of conjugate gradients (Ref. 3) uses the minimum of the grid search as starting point for a modern method of steepest descent to locate the minimum more precisely.

This optimization cycle is repeated at every update time t_ν along the flight trajectory. A flow chart of the scheme in its previous form is given in Fig. 2-5 in which the adjustable parameters are lumped in the parameter vector

$$\vec{K}_i = \begin{bmatrix} \dot{a}_o \\ \dot{a}_1 \\ \dot{g}_2 \end{bmatrix}_i$$

The subscript i denotes the ith iteration of the optimization cycle.

For rapid computing cycles, all simulations during the grid search and gradient search are performed in 1000 times real time. After the optimal set of parameters has been found, the program goes to station ① of Fig. 2-5 where the actual flight is simulated and recorded in real time, using the optimal gain schedules. This simulation stops at the next update time, $t_{\nu+1}$, to repeat the optimization.
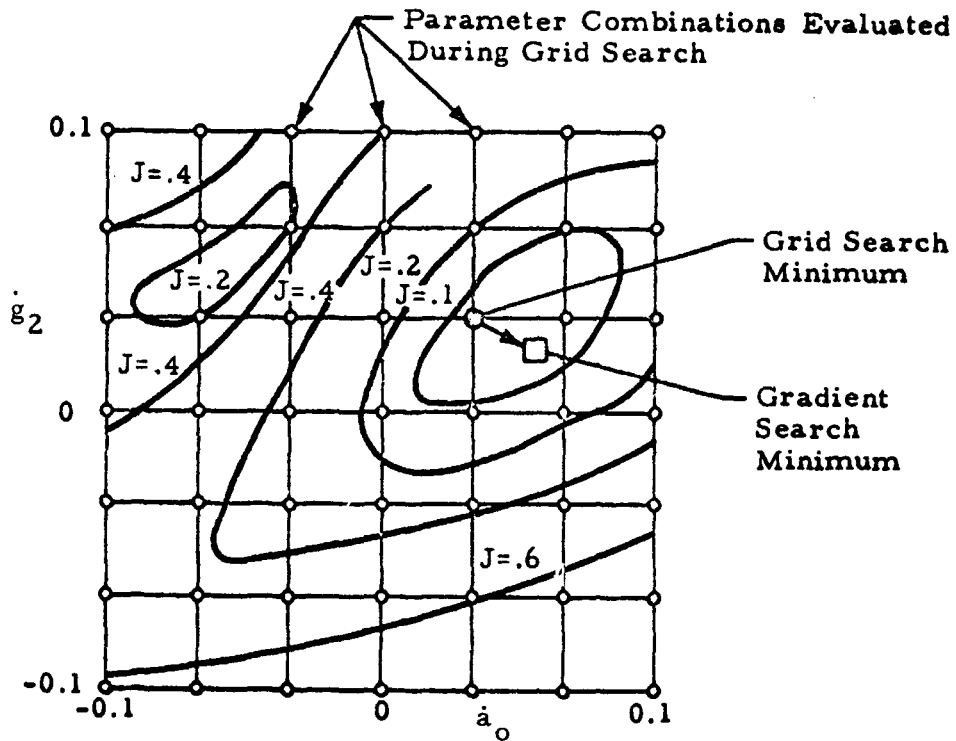
Fig. 2-4 - Parameter Optimization Performed in Two Phases:
(1) Systematic Grid Search (o) for Complete Survey
of Parameter Space; Grid Point of Minimum J (O)
Serves as Starting Point for (2) Gradient Search
Which Locates the Minimum More Precisely (□).
From Grid Search Contour Plots (Lines of J = Const)
Can be Drawn for Better Insight into J-Topology.

START

Initialization and Automatic Checkout

- Set Initial Conditions and Constants
- Set Pots on Analog Computer
- Run Dynamic Check on Analog Computer

Actual Flight Simulation from t_ν to $t_{\nu+1}$

- Read Requirements for Production Run
- ①
- Make Slow Run from t_ν to $t_\nu + \Delta t$. Store State $x(t_\nu + \Delta t)$
- $t_\nu = t_\nu + \Delta t$

Repetitive Simulations from t_ν to $t_\nu + T$ for Grid Search

- Make Fast Run from t_ν to $t_\nu + T$ for all Parameter Combinations of Specified Grid. Compute, Store and Print Out Performance Indices $J(\overline{K}_i)$
- Use Parameters $\overline{K}_i$ of J_{min} to Initialize Gradient Search

---

- $i = 1$
- Compute Gradient $\overline{\nabla} J(\overline{K}_i)$
- ②
- $H_i = I$ (Unit Matrix)
- ③
- Compute $\overline{s}_i$ and η_i
- Is $\eta_i > 1$? — YES → $\eta_i = 1$
  - NO
- ④
- $\overline{K}_i^* = \overline{K}_i + \eta_i \overline{s}_i$
- Compute $J(\overline{K}_i^*)$ and $\overline{\nabla} J(\overline{K}_i^*)$
- Fit Cubic Curve Through $\overline{K}_i$ and $\overline{K}_i^*$

- Compute Step Size $\overline{\sigma}_i = a \overline{s}_i$ from $\overline{K}_i$ to Minimum of Cubic Curve at $\overline{K}_{i+1} = \overline{K}_i + \overline{\sigma}_i$
- Compute $J(\overline{K}_{i+1})$
- Is $J(\overline{K}_{i+1}) < J(\overline{K}_i)$ and $< J(\overline{K}_i^*)$?
  - YES → Compute $\overline{\nabla} J(K_{i+1})$ → $J(\overline{K}_i) = J(\overline{K}_{i+1})$, $\overline{\nabla} J(\overline{K}_i) = \overline{\nabla} J(\overline{K}_{i+1})$
  - NO
- Is $J(\overline{K}_i^*) < J(\overline{K}_i)$ and $< J(\overline{K}_{i+1})$?
  - NO → Have N Attempts Been Performed in One Iteration ?
    - YES → $\eta_i = .4 \eta_i$ → ④
    - NO
    - Is $i \geq i_{max}$? — YES → **STOP**
      - NO
      - $\epsilon = 2\epsilon$, $i = i + 1$ → ②
  - YES → $J(\overline{K}_i) = J(\overline{K}_i^*)$, $\overline{\nabla} J(\overline{K}_i) = \overline{\nabla} J(\overline{K}_i^*)$
- Is $[\overline{\nabla} J(\overline{K}_i)^T \overline{\nabla} J(\overline{K}_i)] \leq \epsilon$?
  - NO
  - Is $i \geq i_{max}$?
    - NO → $i = i + 1$ → Compute H_i → ③
    - ①

Fig. 2-5 · Flow Chart of Hybrid Computer Optimization Scheme for Minimization of the Multivariable Performance Criterion $J(\overline{K})$

LMSC/HREC D162122-I
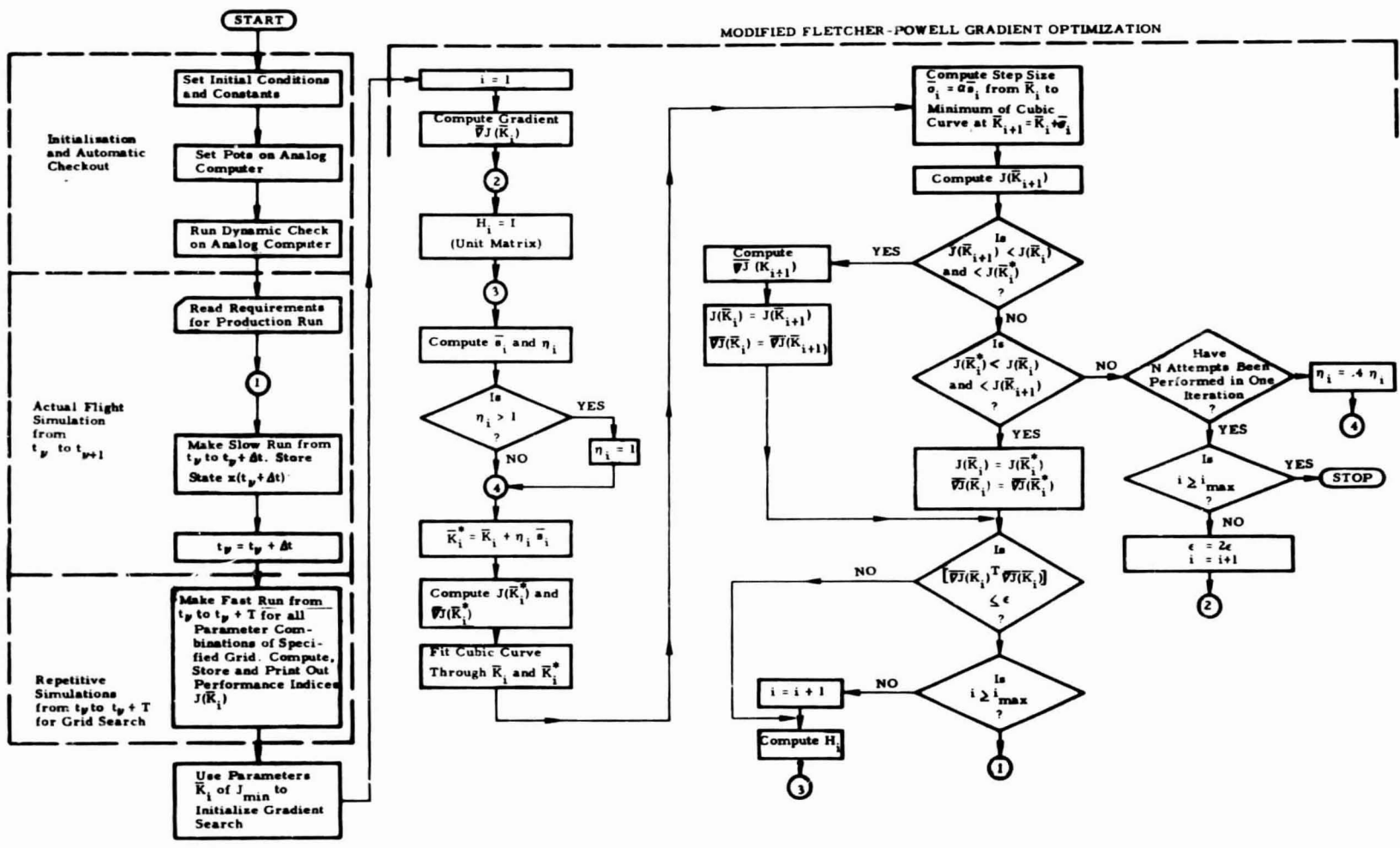
2.2 SIMULTANEOUS CONSIDERATION OF TWO ADVERSE FLIGHT CONDITIONS

The optimization scheme was modified to consider simultaneously two extreme flight conditions during optimization, such as failure of a windward engine as well as failure of a leeward engine at a common failure time. In the load relief design study, bending loads are observed at two stations along the vehicle, where only the peak value is used in the performance index to be minimized. The resulting gain schedule will therefore minimize the peak bending load measured at one of the two stations if either possible failure mode occurs.

The modifications that were made are indicated in Blocks A, B, and C of Fig. 2-6, which is an updated version of Fig. 2-5.

BLOCK A: Grid Search Modification

(1) A grid point n is chosen.

(2) One fast run made for failure A for gain slopes $(K_i)_n$.

(3) Peak moment, gain slopes and $J_A(K_i)_n$ stored temporarily.

(4) One fast run made for failure B for gain slopes $(K_i)_n$.

(5) Peak moment, gain slopes and $J_B(K_i)_n$ stored temporarily.

(6) Maximum peak moment of (3) and (5) stored. Associated gain slopes and $J(K_i)_n$ stored.

(7) Grid search moves to next grid point, $n+1$.

(8) Repeat (2) through (6) and continue to (9)

(9) $J(K_i)_n$ of previous (6) compared to $J(K_i)_{n+1}$ of (6) just completed.

(10) Minimum $J(K_i)$ of (9) and associated gain slopes stored.

(11) Repeat (8) until total grid has been searched.

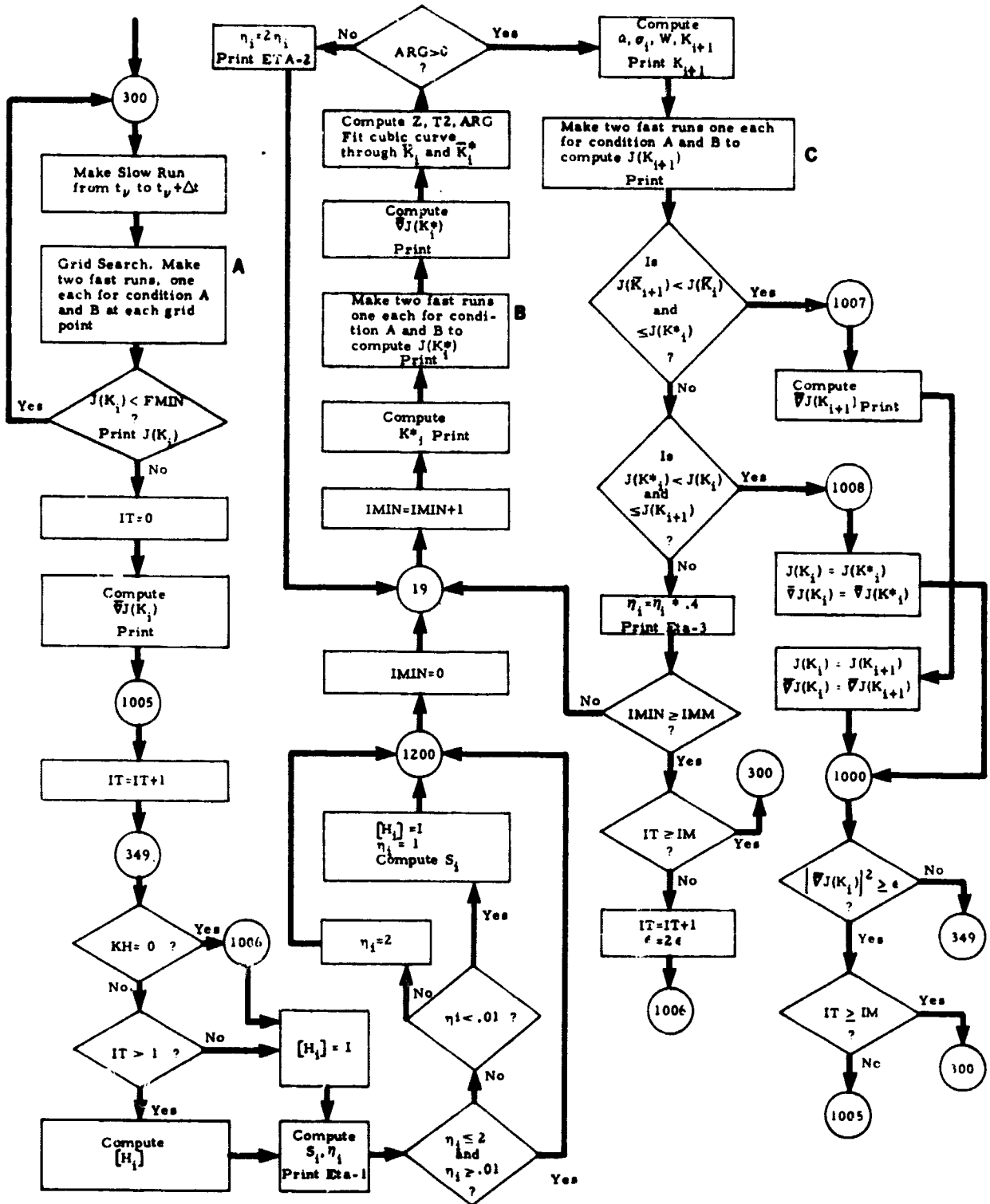(12) Gain slopes of (10) used to initiate gradient search.

Fig. 2-6 - Flow Chart of Minimization Scheme Based on Fletcher and Powell
(Ref. 3), Extended for Grid Search Preceding Gradient Search.
Performance Index J Depends upon two Dynamic Simulations
(Condition A and Condition B).

BLOCK B: Modification to $J(K_i^*)$ Computation

(1.) One fast run made for failure A for gain slopes K_i^*.

(2.) Peak moment, gain slopes and $J_A(K_i^*)$ stored temporarily.

(3.) One fast run made for failure B for gain slopes K_i^*.

(4.) Peak moment, gain slopes and $J_B(K_i^*)$ stored temporarily.

(5.) Maximum peak moment of (2.) and (4.) stored. Associated gain slopes and $J(K_i^*)$ stored.

(6.) $\overline{\nabla}J(K_i^*)$ computed and gradient search continued. The computation of $\overline{\nabla}J(K_i)$ considers only one failure case, that is, the case that has been determined to produce the maximum peak moment for the gain slopes, K_i. This is justifiable because perturbations of K_i used to compute $\overline{\nabla}J(K_i)$ are small enough to cause only minor changes in the peak moments of each case if both cases are considered. The same conditions also hold true for the computation of $\overline{\nabla}J(K_i^*)$.

BLOCK C: Modification of $J(K_{i+1})$ Computation

(1.) One fast run made for failure A for inputs K_{i+1}.

(2.) Peak moment, gain slopes and $J_A(K_{i+1})$ stored temporarily.

(3.) One fast run made for failure B for inputs K_{i+1}.

(4.) Peak moment, gain slopes and $J_B(K_{i+1})$ stored temporarily.

(5.) Maximum peak moment of (2.) and (4.) stored. Associated gain slopes and $J(K_{i+1})$ stored.

(6.) Gradient search continues.

Flow charts of these modifications are shown in Figs. 2-7, 2-8, and 2-9.

2.3 SEQUENCE OF COMPUTATIONS

The modified optimization technique created a problem in the form of excessive computer usage. After the optimization process is completed at a certain update time t_ν along the flight trajectory, two real time simulations
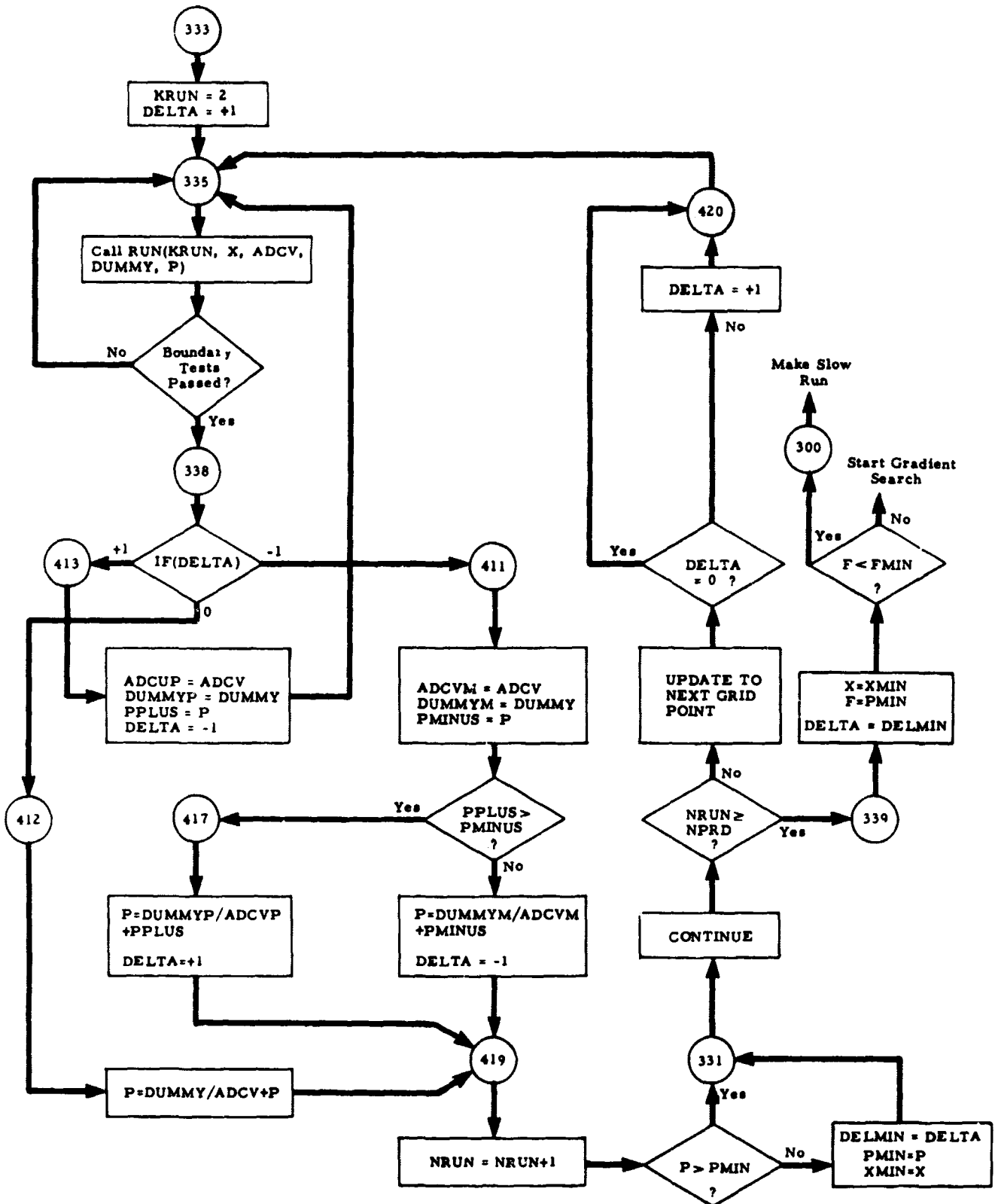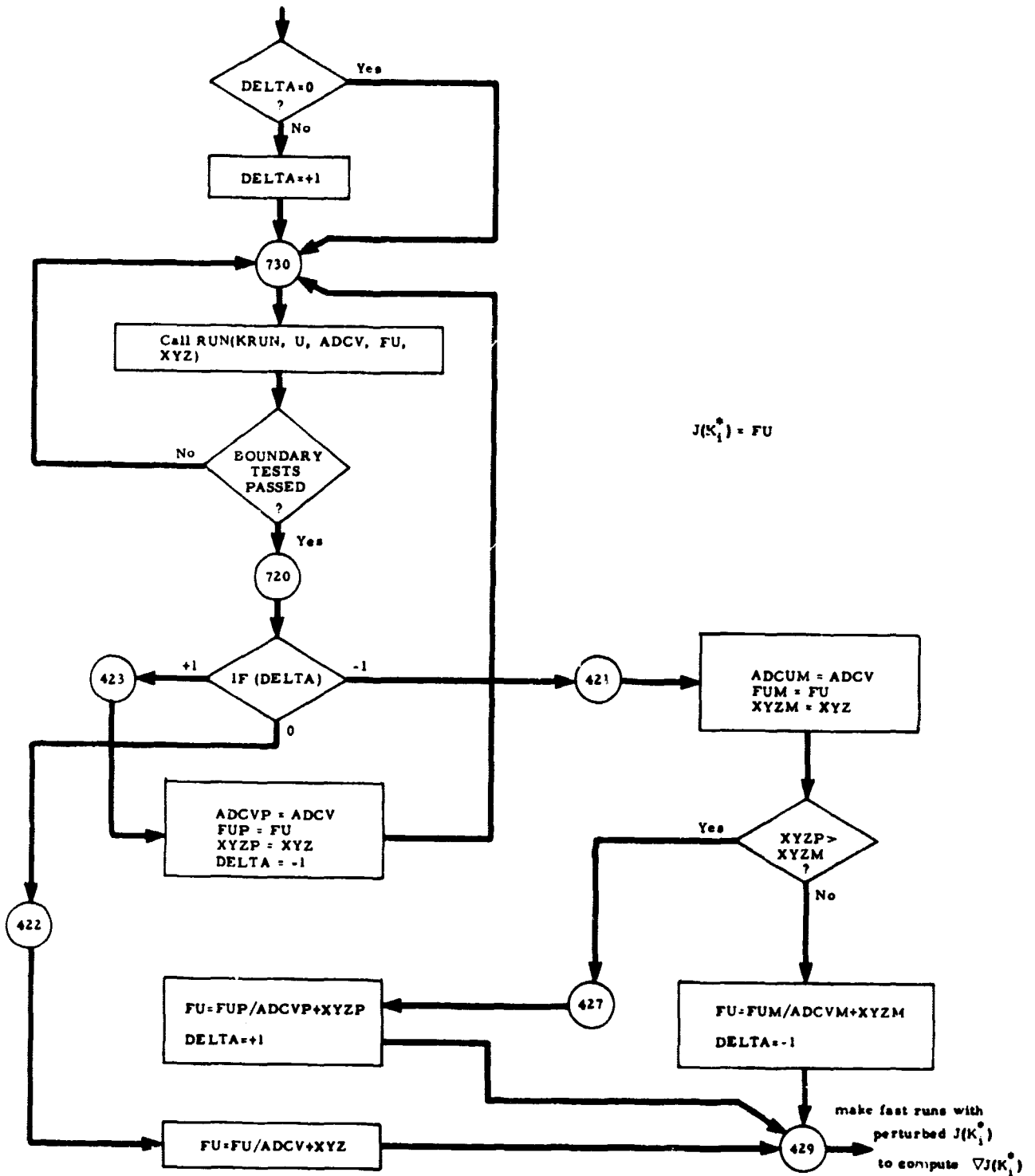
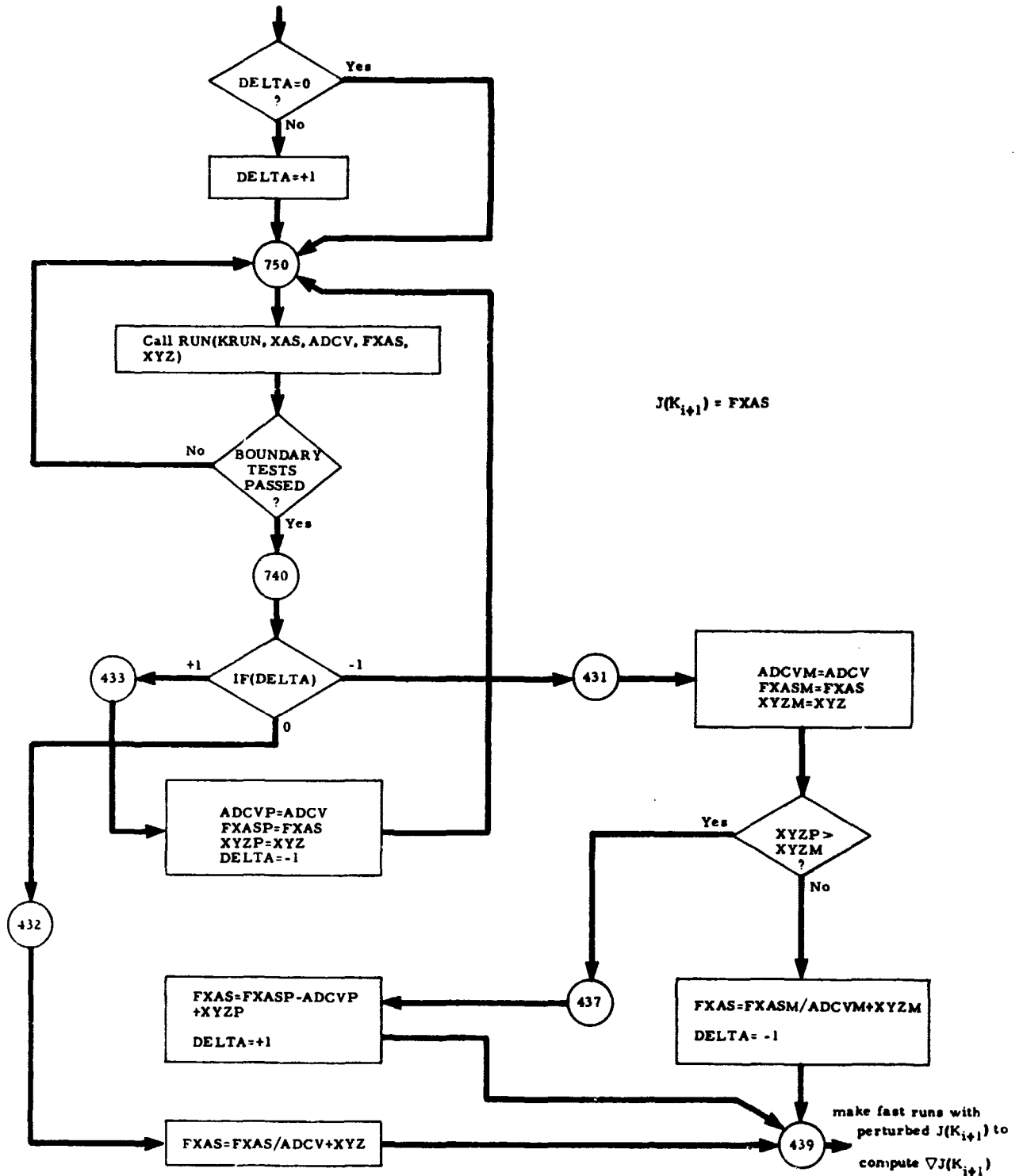Fig. 2-7 - Grid Search Flow Chart

Fig. 2-8 - Computation of $J(K_i^*)$

Fig. 2-9 - Computation of $J(K_{i+1})$

should be performed for the optimized interval $(t_\nu, t_{\nu+1})$ and recorded on different recorders.

Since only one remote control recorder was available and the necessary track and store units were not available, computations previously followed the less efficient sequence of Chart 2-1, where it was necessary to repeat the complete optimization since only one failure case could be recorded per optimization.

This lack of efficiency prompted the modifications shown in Chart 2-2. The optimized gain slopes and the time at which they occur are stored and punched on data cards at the end of the flight assuming a windward engine failure (Case A). These data with the use of digital logic are used to rerun the flight assuming a leeward engine failure (Case B) without optimization.

This modification of the computation sequence represents an approximate saving of 50% in computer time.

(A) Optimization with Simulation
    of Case A

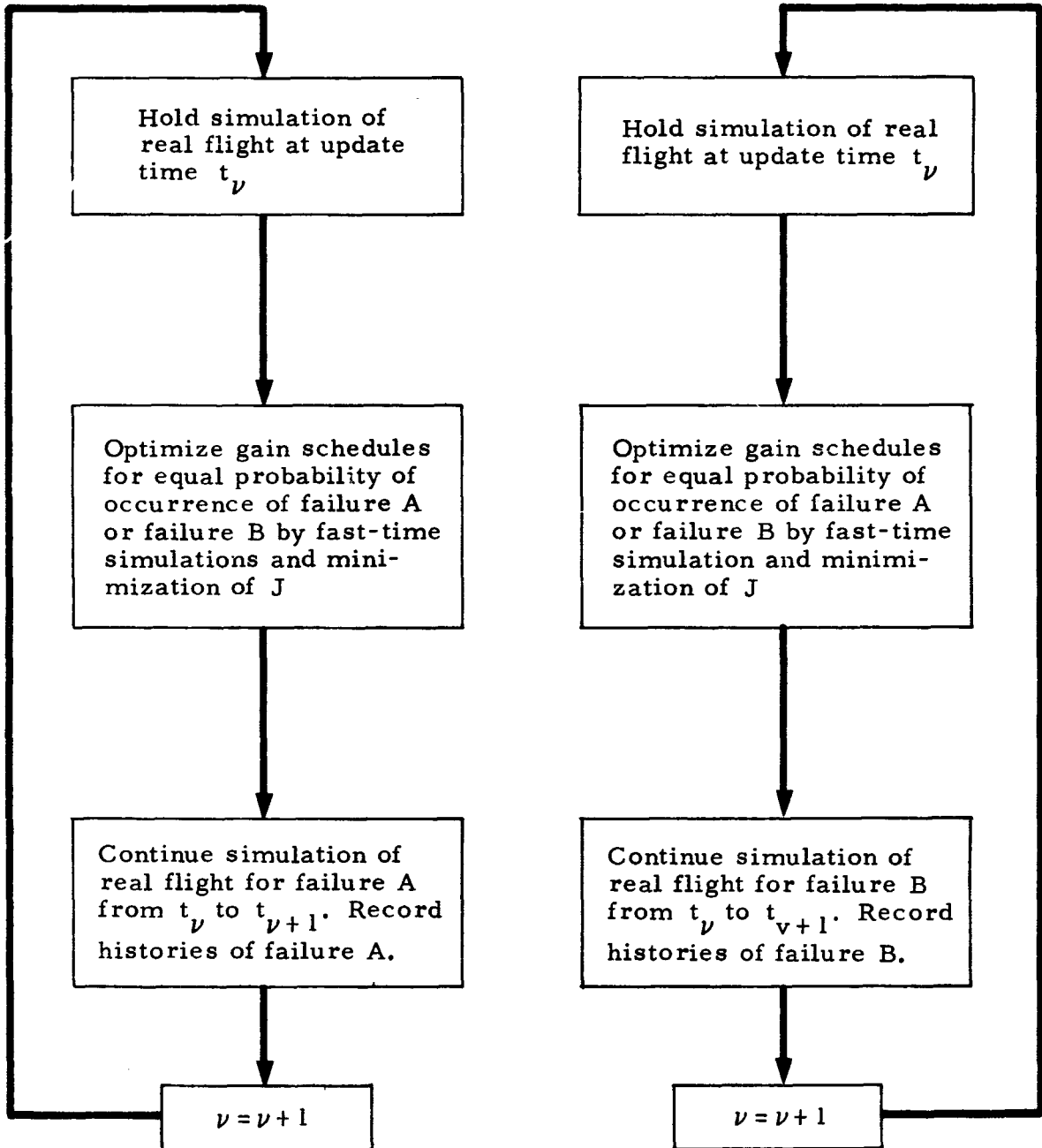(B) Repeated Optimization with
    Simulation of Case B

```
┌─────────────────────────┐     ┌─────────────────────────┐
│ Hold simulation of      │     │ Hold simulation of real │
│ real flight at update   │     │ flight at update time t │
│ time  t                 │     │                        ν│
│         ν               │     │                         │
└─────────────────────────┘     └─────────────────────────┘

┌─────────────────────────┐     ┌─────────────────────────┐
│ Optimize gain schedules │     │ Optimize gain schedules │
│ for equal probability of│     │ for equal probability of│
│ occurrence of failure A │     │ occurrence of failure A │
│ or failure B by fast-time│    │ or failure B by fast-time│
│ simulations and mini-   │     │ simulation and minimi-  │
│ mization of J           │     │ zation of J             │
└─────────────────────────┘     └─────────────────────────┘

┌─────────────────────────┐     ┌─────────────────────────┐
│ Continue simulation of  │     │ Continue simulation of  │
│ real flight for failure A│    │ real flight for failure B│
│ from t  to t   .  Record│     │ from t  to t    .  Record│
│      ν      ν+1         │     │      ν      v+1         │
│ histories of failure A. │     │ histories of failure B. │
└─────────────────────────┘     └─────────────────────────┘

        ┌──────────┐                    ┌──────────┐
        │ ν = ν+ 1 │                    │ ν = ν+ 1 │
        └──────────┘                    └──────────┘
```

Chart 2-1 – Previous Sequence of Computations. Optimization Process
       is Repeated to Obtain Recordings of Both Flight Conditions

(A) Optimization with Simulation of Case A

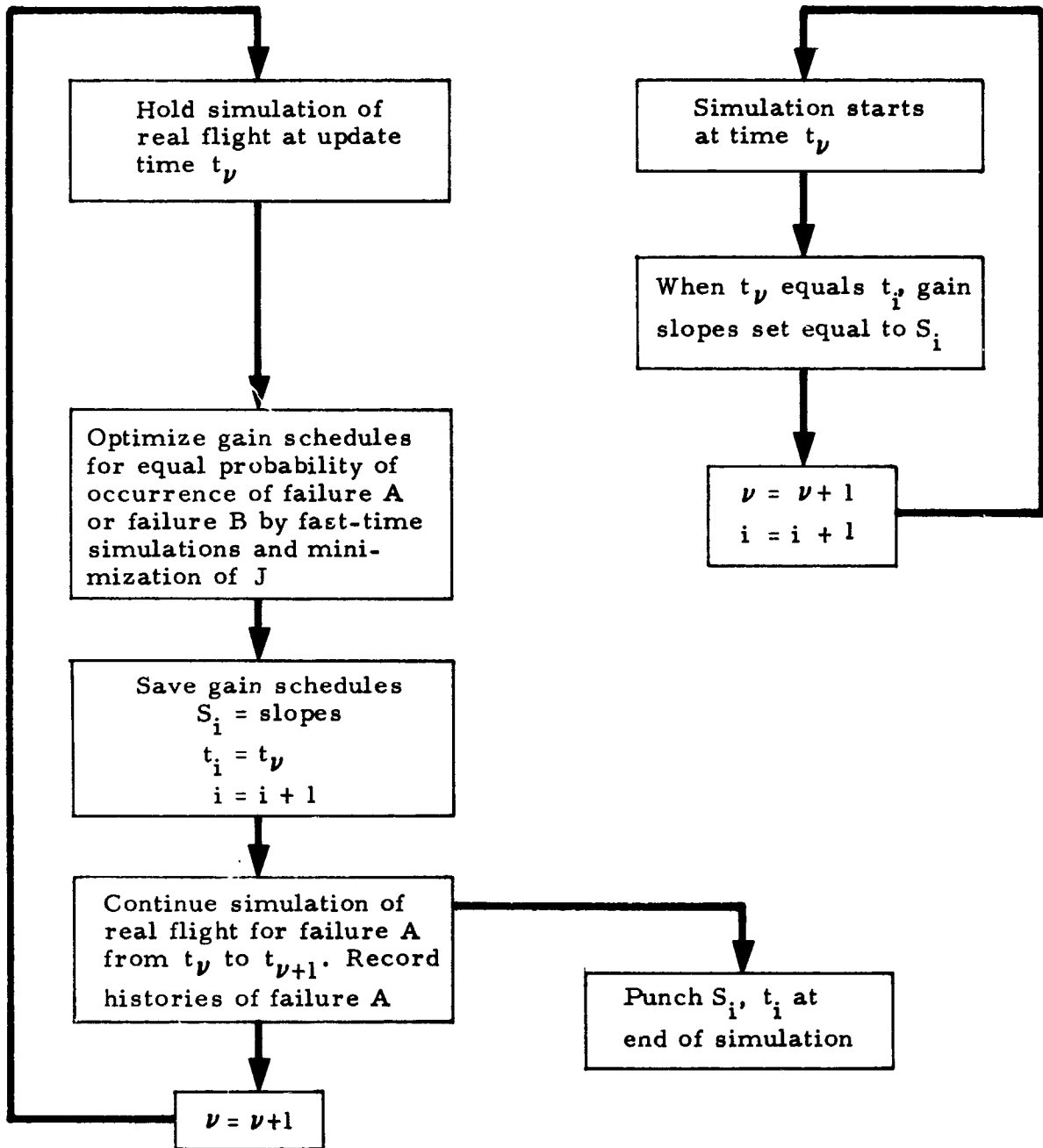(B) Repeated Run for Simulation of Case B (Optimization not Repeated)

Hold simulation of real flight at update time t_ν

Optimize gain schedules for equal probability of occurrence of failure A or failure B by fast-time simulations and minimization of J

Save gain schedules
S_i = slopes
$t_i = t_\nu$
$i = i + 1$

Continue simulation of real flight for failure A from t_ν to $t_{\nu+1}$. Record histories of failure A

$\nu = \nu + 1$

Simulation starts at time t_ν

When t_ν equals t_i, gain slopes set equal to S_i

$\nu = \nu + 1$
$i = i + 1$

Punch S_i, t_i at end of simulation

Chart 2-2 – Modified Sequence of Computations. Optimized Gain Schedules are Stored During Optimization to be Used in Simulation of Second Flight Condition. No Repetition of Optimization Process Required.

Section 3
STUDY RESULTS

3.1 CRITICAL EVALUATION OF MODIFIED SCHEME

To evaluate the operation and performance of the modified system, production runs were made where $\dot{a}_o$ and $\dot{g}_2$ were optimized and a_1 was held constant. In a first test case the optimization considered the two most adverse failure conditions, failure of a leeward engine or failure of a windward engine at 76 sec. In this and all subsequent examples, the wind profile used is shown at the top of Fig. 1-1, page 1-2, with its peak and a superimposed gust at 74 sec.

Results of this optimization are presented in Figs. 3-1 through 3-3 and compared with the loads which would result from the nominal Saturn V control gains. The following data and notations were used in the example:

Start of simulation	40 sec
Start of optimization	50 sec
Optimization look-ahead interval, T	20 sec
Peak wind time (and start of gust)	74 sec
Initial attitude error feedback gain, a_o	0.9
Initial accelerometer feedback gain, g_2 $\left(\deg/\dfrac{m}{sec^2}\right)$	0.0
Constant error rate feedback gain, a_1 (sec)	0.67 sec

End of simulation	98 sec
Weighting factor for stability term in performance index q	0.05
Failure time, Case A (Windward engine out)	76 sec
Failure time, Case B (Leeward engine out)	76 sec

The constant gain simulations lead to peak loads of 21% and 26% of the structural limit $\overline{M}_B$ at Stations 1 and 3, respectively, for failure A (Fig. 3-1a) and to 51% at both stations for failure B (Fig. 3-2a).

The optimization simulations result in slightly higher peak load magnitudes (33% and 36% of $\overline{M}_B$), for failure A (Fig. 3-1b). Peak loads for the worst bending load, Case B, however, are reduced to 36% and 35% as shown in Fig. 3-2b. A near-perfect tradeoff of possible bending load peaks is thus obtained, as illustrated again in Fig. 3-4, where the most critical peaks are sharply reduced at the expense of less severe minor peaks. All possible peaks of the optimized system for failure A as well as for failure B lie within a narrow band of 33% to 36% of the structural limit $\overline{M}_B$ of the respective stations. These results demonstrate that sensitivity to specific failure modes is indeed eliminated by the modifications made. The gain adjustment strategy reduces the worst load among all the failure cases and all the load stations considered. The resulting optimal gain schedules represent the best tradeoff in load relief with respect to possible occurrence of any one of the two failure modes considered. The load reductions achieved are due to two factors: (1) addition of an accelerometer feedback channel and (2) time-varying gain schedules determined through the optimization program.

To assess the contribution of the first factor to the total load reductions achieved, a series of simulations was made with accelerometer feedback and constant gains. The best results were obtained with the following gain adjustments:
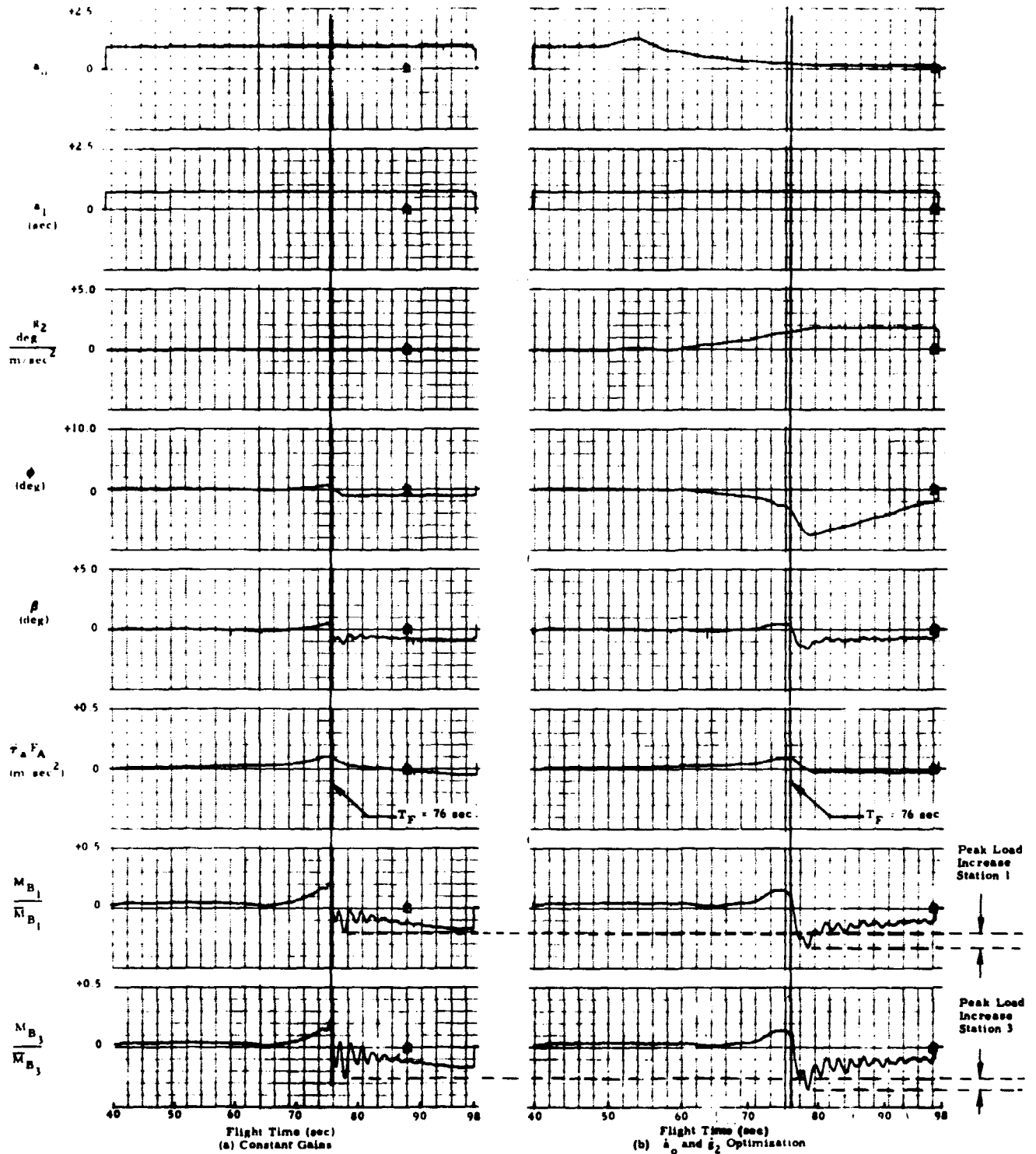
Fig. 3-1 - Time Histories of Typical Optimization Run (Fig. 3-1b) Compared With Constant Gain Case (Fig. 3-1a).
Windward Engine Fails in Both Cases at $T_F = 76$ sec. Windward or Leeward Engine Failure is Considered
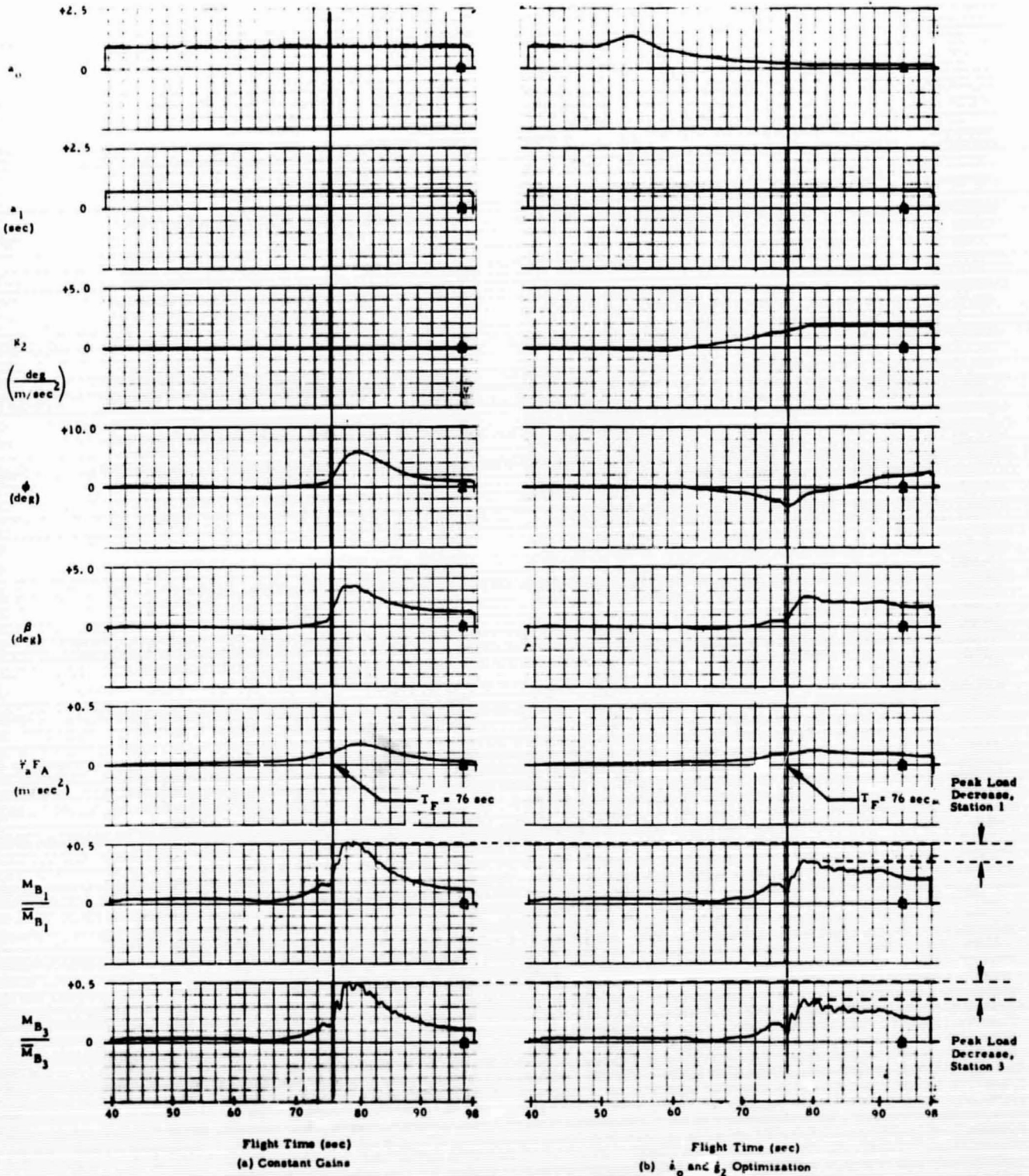With Equal Probability.

Fig. 3-2 - Time History of Optimization Run Identical to (Fig. 3-1b) Except for Failure Mode: Leeward Engine Fails at T_F = 76 sec. Worst Load Peaks (Fig. 3-2a) are Substantially Reduced (Fig. 3-2b) Due to Gain Optimization.
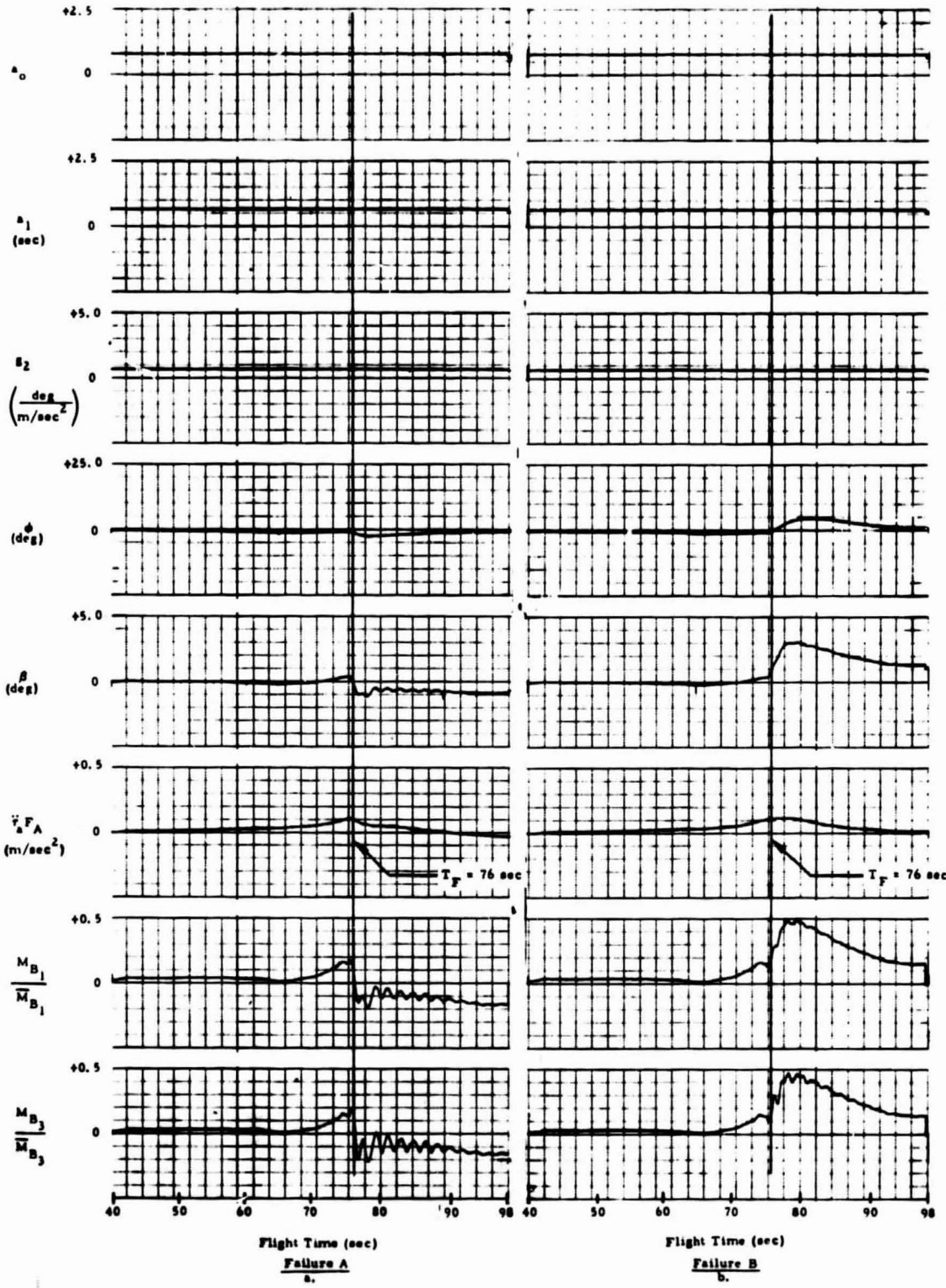
Fig. 3-3 - Flight Histories for Constant Gains $a_0 = 0.8$, $a_1 = 0.67$, $g_2 = 0.7$, Including Accelerometer Feedback
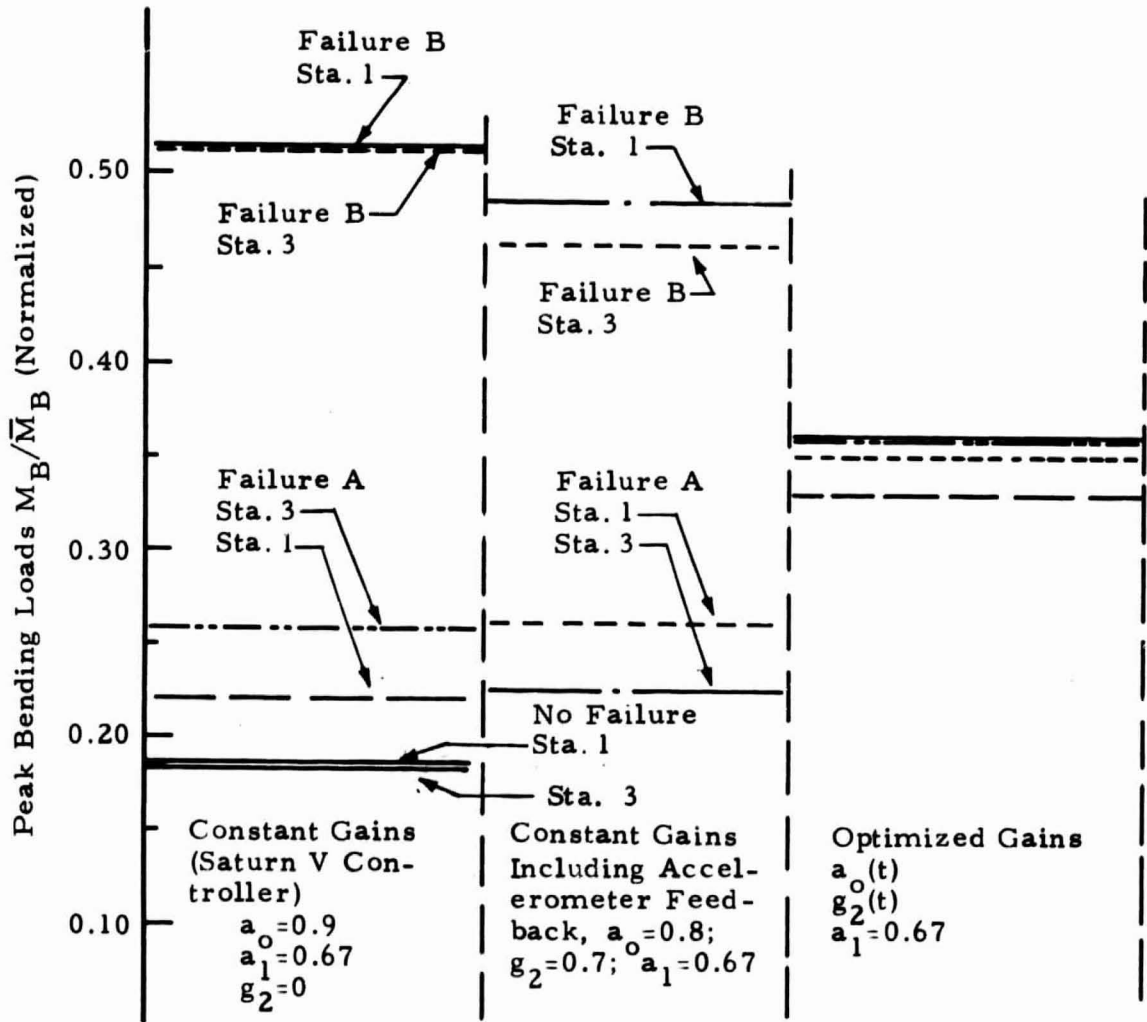
Fig. 3-4 - Peak Bending Loads Compared for Constant Gain Case
and for Case Optimized for Failure of Leeward or
Windward Engine at 76 Seconds

$$a_o = 0.8; \quad a_1 = 0.67 \text{ sec}; \quad g_2 = 0.7^o/\text{m/sec}^2$$

These values are the average gains of the optimized schedules shown in Figs. 3-1b and 3-2b. Figure 3-3 represents the resulting flight histories for failure A and failure B.

The peak bending loads are included in the plot, Fig. 3-4, which compares the constant gain loads with the reduced loads due to the optimization. This comparison readily shows that the major contribution to the load reductions is due to the optimal time-varying adjustments. Addition of an accelerometer feedback alone helps little to reduce loads in this severe case.

3.2 VARIATIONS IN ENGINE FAILURE TIME

Figure 3-5 represents the results of a systematic variation of failure time for both types of engine failures during the most critical flight time around the peak wind, max $q\alpha$, and max q. Failure times considered were 66, 69, 71, 74, 76, 81, 86 and 91 sec. Other conditions were:

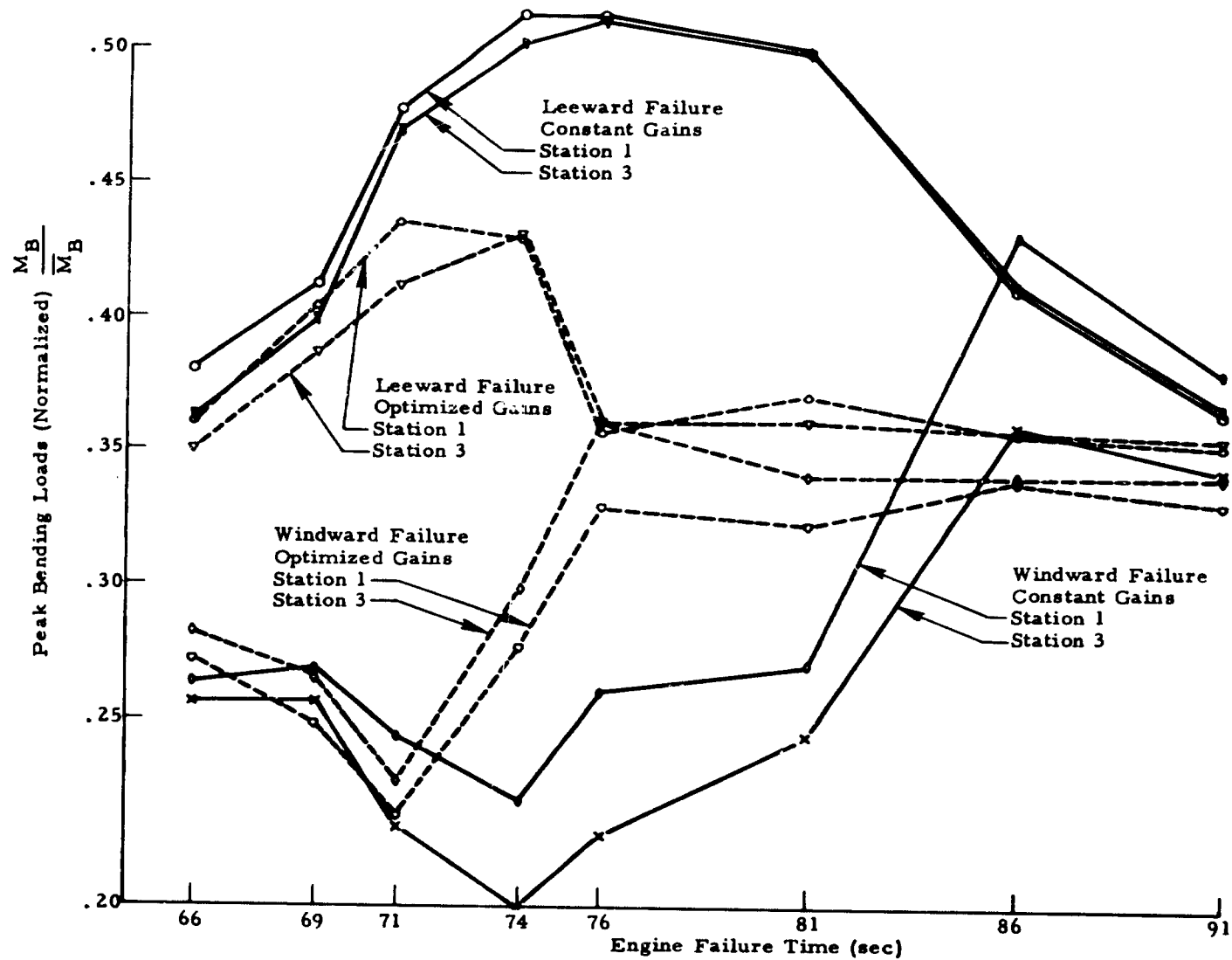|	
Start of simulation	40 sec
Start of optimization	50 sec
Optimization look-ahead interval T	20 sec
Wind profile of Fig. 1-1 with peak wind time (and start of gust)	74 sec
Initial gain a_o	0.9
Initial gain g_2 (deg/m/sec^2)	0.0
Constant gain a_1 (sec)	0.67 sec

Fig. 3-5 - Peak Bending Load Comparison of Constant Gain Case and for Optimized
Gain Case at Various Engine Failure Times. Windward and Leeward
Engine Failures Considered with Equal Probability

End of simulation	98 sec
Weighting factor for stability term in performance index q	0.05

Figure 3-5 shows that the optimization scheme computes the best tradeoff in load relief with respect to possible occurrence of either one of the two failure modes. The efficiency of the scheme is a function of the failure time as related to the peak wind and gust at 74 sec. Note that the efficiency is lowest in the region just prior to occurrence of the peak wind and is at its highest efficiency after the peak wind. Possible reasons for this problem were explored, but no significant increase in efficiency without sacrificing system stability was possible.

An attempt was made to use the gain schedules obtained from this systematic failure study to determine general gain schedules that would minimize peak bending loads at any possible failure time. It was expected that these general gain schedules would have reduced the peak bending loads as shown in Fig. 3-5 to a region between the 35% to 40% of the structural limits obtained by the optimized system and the over 50% for some of the non-optimized cases. Although the sensitivity to the type of engine failure had been eliminated, it became apparent rather quickly that any deviation from the optimized gain schedules for a particular failure time when applied to another failure time caused rather drastic changes in the disturbance history. In fact, in most cases, the disturbance histories were worse than those for constant gain control.

There was not enough time to work out more satisfactory ways to derive generally valid sub-optimal gain schedules from a series of schedules optimized for different failure histories. If further efforts using conventional control engineering tools should fail, the optimization method could be extended to cope with more than two flight or failure conditions. In the present load relief example, such events as leeward engine failure, windward

engine failure or no failure might be included in the design. This should reduce the sensitivity of the optimal design to failure uncertainties even more and facilitate the averaging of similar gain schedules to achieve generally valid designs.

3.3 PERFORMANCE UNDER NOMINAL CONDITIONS

Figure 3-6 represents a series of runs to evaluate the performance of the optimizer under nominal Saturn V conditions. This series of runs included:

- Optimization for nominal flight without failure

- Simulation of flight histories for constant g_2

- Simulation of flight histories for nominal flight without failure, using gain schedules which were optimized for engine failures occurring at various flight times.

Optimization for nominal flight conditions without the occurrence of an engine failure results in peak moment reductions of 18% to 14% and 17.5% to 13% for station 1 and 3, respectively.

Simulation of flight histories for constant accelerometer feedback g_2 for a failure time of 76 sec yielded results only slightly better than those for nominal Saturn V control gains where $g_2 = 0$. For failure B, peak moments were reduced from 51% to 48% and from 51% to 47% of the structural limits for stations 1 and 3, respectively. For failure A, peak moments were increased from 19% to 20.5% and from 22% to 25% of the structural limits for stations 1 and 3, respectively.

Optimal gain schedules previously obtained from the series of systematic studies represented by Fig. 3-5 were each run assuming that no failure would occur. The peak bending loads for both station 1 and 3 are shown in Fig. 3-6. It is evident that these schedules are not optimized for a no-failure case, since the majority of the bending moments exceed those for the constant gain case.
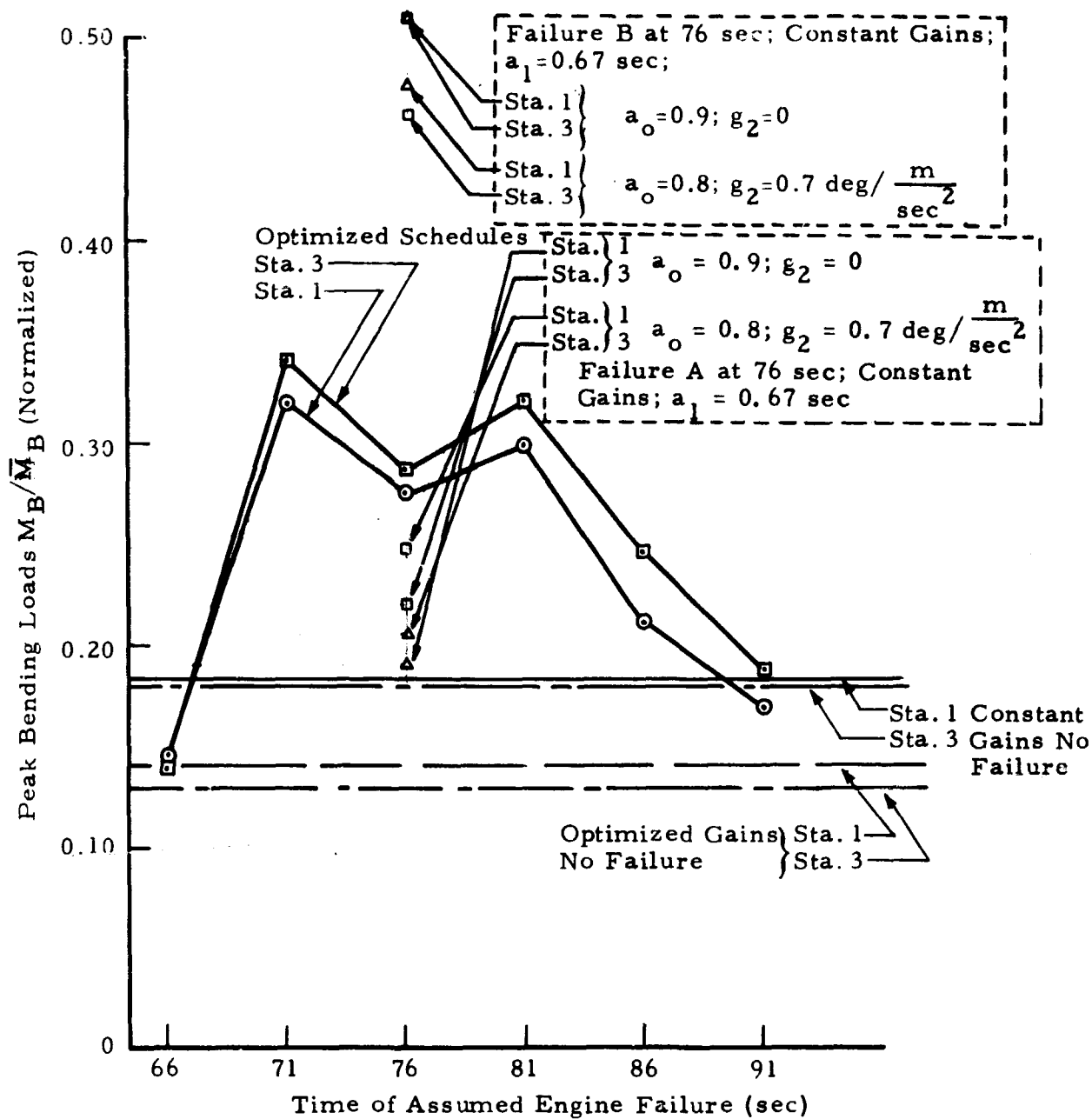
Fig. 3-6 – Comparison of Saturn V Performance Under Nominal and
Failure Conditions

3.4   THREE-GAIN OPTIMIZATION

A three-parameter ($\dot{a}_o$, $\dot{a}_1$ and $\dot{g}_2$) optimization was run with a failure
time of 76 sec. The optimization considered the occurrence of a leeward
or windward engine failure. Figures 3-6 and 3-7 show the results of this
run. When results were compared, peak loads at all the load stations were
found to be approximately 2 to 4% less than the peak loads of the two-
parameter optimization ($\dot{a}_o$, $\dot{g}_2$).

Conditions of the simulation were:

Start of simulation	40 sec
Start of optimization	50 sec
Optimization look-ahead interval	20 sec
Peak wind time (and start of gust)	74 sec
Initial gain a_o	0.9
Initial gain g_2 (deg/m/sec^2)	0.0
Initial gain a_1 (sec)	0.67 sec
End of simulation	98 sec
Weight factor for stability term in performance index (q)	0.05

By including the rate gain (a_1) in the optimization process, the possibility
of an unstable configuration is increased. Note that the general trends of
a_o and g_2 for the three-gain optimization are the same as those for the two-
gain optimization of Figs. 3-1 and 3-2. Very little is gained by scheduling the
rate-feedback (about 4% more load reduction). Thus earlier observations
were verified that rate gain scheduling is not efficient in load-relief con-
troller design and all results obtained by optimal adjustments of $a_o(t)$ and
$g_2(t)$ are very close to the true optimum with three-gain-scheduling of $a_o(t)$;
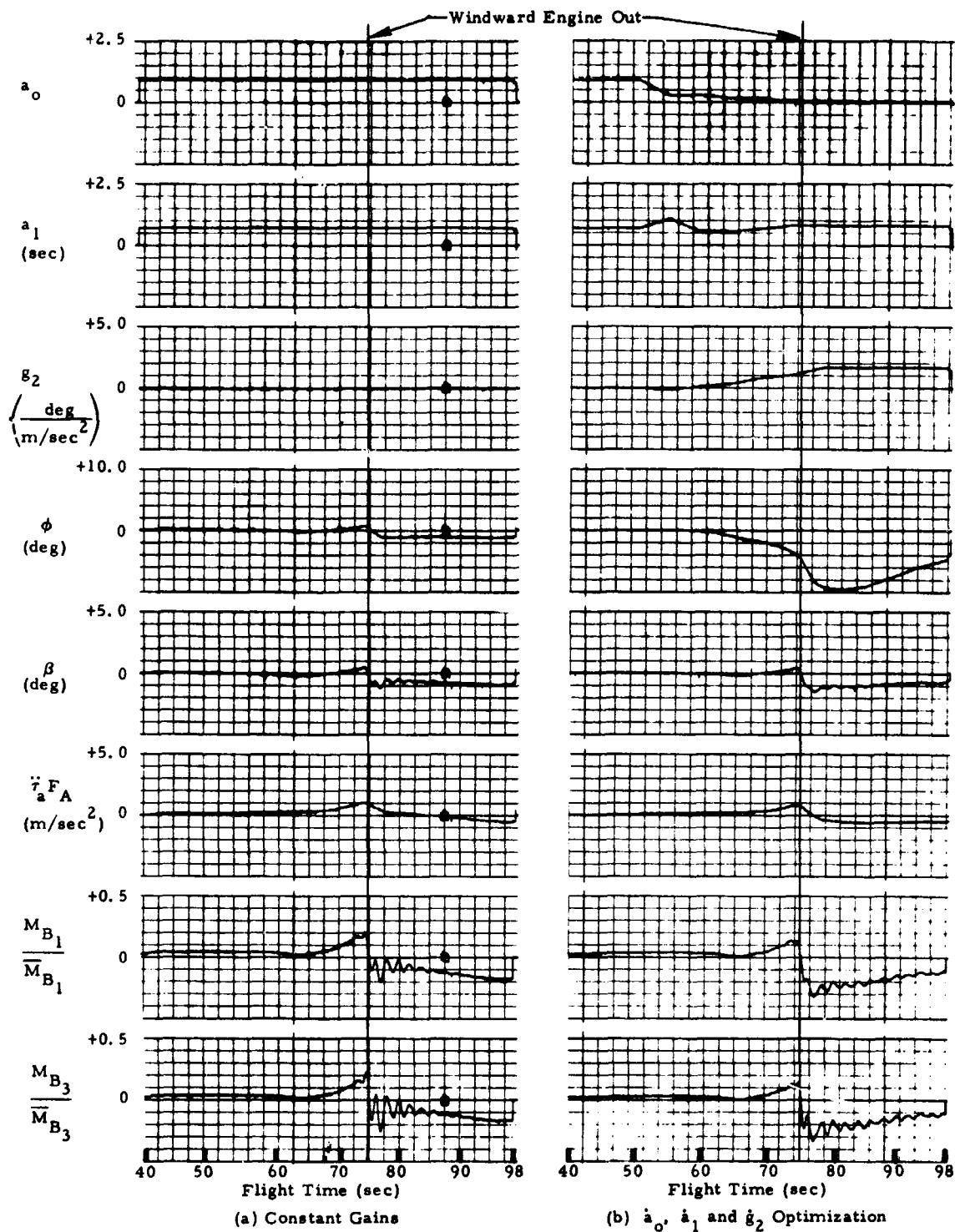$g_2(t)$; and $a_1(t)$.

Fig. 3-7 - Time Histories of Typical Optimization Run (Fig. b) Compared with Constant
Gain Case (Fig. a). Optimization based on Possible Windward or Leeward
Engine Failure Recordings Show Effects of Windward Engine Failure: Peak
Loads are slightly increased.

Leeward Engine Out

a_o

+2.5

0

+2.5

a_1
(sec)

0

+5.0

g_2

$\left(\dfrac{deg}{m/sec^2}\right)$

0

+10.0

ϕ
(deg)

0

+5.0

β
(deg)

0

+5.0

$\ddot{r}_a F_A$
(m/sec^2)

0

+0.5

$\dfrac{M_{B_1}}{\overline{M}_{B_1}}$

0

+0.5

$\dfrac{M_{B_3}}{\overline{M}_{B_3}}$

0

40   50   60   70   80   90   98   40   50   60   70   80   90   98

Flight Time (sec)   Flight Time (sec)

(a) Constant Gains   (b) $\dot{a}_o$, $\dot{a}_1$, and $\dot{g}_2$ Optimization
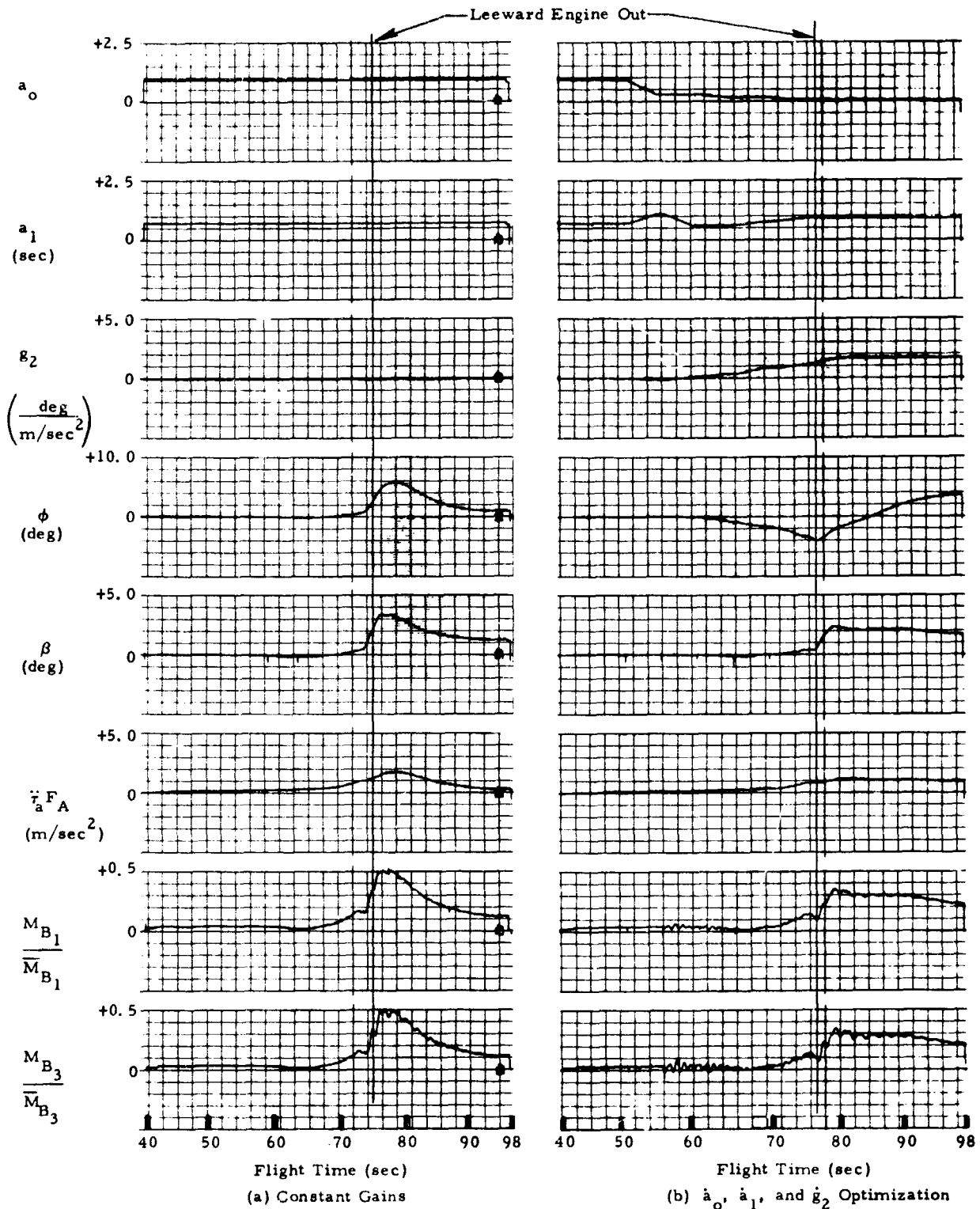
Fig. 3-8 - Time Histories of Same Optimization Run as in Fig. 3-7. Recordings show
the Effects of a Leeward Engine Failure: Worst Load Peaks of (Fig. a) are
substantially Reduced (Fig. b) Due to Gain Optimization. However, Load
Reduction is only 4% Better than Fig. 3-2 where a_1 was kept Constant.

Section 4
CONCLUSIONS AND RECOMMENDATIONS

4.1 CONCLUSIONS

A new computerized design tool applicable to complex optimal control problems was developed during previous contracts and refined under the present study. The specific application studied was the optimal adjustment of the Saturn V first-stage attitude control system so that peak bending loads caused by wind forces and critical engine failures are minimized.

The major shortcoming of the optimization method in its earlier form and for practically all other time-domain optimizations was that the optimal gain schedules were highly sensitive to the specific flight and failure condition assumed. The major refinement accomplished during this study was to extend the method to simultaneously cope with more than one flight condition. This refinement was highly successful in substantially reducing this sensitivity to specific flight conditions, making the optimization method a useful and efficient computerized design tool characterized by these features:

- The variational problem of finding optimal time-varying control gains is reduced to a sequence of parameter searches which result in piecewise linear near-optimal gain schedules rapidly determined by hybrid computing techniques.

- System dynamics and flight environment including non-linear effects, wind disturbances and critical failures can be realistically represented and accounted for in the design.

- The engineer's design goal can be specified in a very direct way since there are virtually no constraints as to the mathematical form of the performance measure.

• The sensitivity of the optimal control gain schedules to
specific flight conditions is substantially reduced by con-
sidering a multiple of possible flight conditions during the
design rather than tuning the control system to one isolated
environmental condition.

4.2   RECOMMENDED STABILITY ANALYSIS STUDIES

All these highly desirable characteristics could be gained only by
deviating from the grounds of optimal control theory. While linear optimal
control theory guarantees stability of the optimal solution at least for con-
stant coefficient systems without external disturbances, no such guarantees
exist for the more important class of most aerospace systems with time-
varying coefficients and external disturbance inputs.

Preliminary studies indicate that a stability analysis scheme could be
developed and incorporated into the present hybrid optimization program.
The scheme would be based on Lur'e's canonical form and Lyapunov stability
theory. It would establish admissible regions for the adjustable parameters
which guarantee stability. The existing optimization program can then be
readily modified to restrict the search for optimal parameters to these ad-
missible regions. Stability of the optimized system would thus be assured
and the search for optimal parameters could be speeded up at the same time.

Lockheed therefore recommends that advanced stability analysis tech-
niques be developed to be used in connection with the present optimization
program. This would further enhance the practicality of the method as a
design tool and would make it a candidate for possible future onboard appli-
cations in an adaptive system where assured stability at all times is a
necessity.

4.3 POTENTIAL APPLICATIONS TO OTHER OPTIMIZATION PROBLEMS

Application studies to date were restricted to the booster load relief problem with emphasis on failure mode effects. In its new expanded form, the optimization scheme is sufficiently versatile, however, to be applied to a number of other complex design problems with minor or no modifications required. Promising application areas are:

- **Optimal Controller Design Insensitive to Wind Variations.**
  If wind disturbances represent the major uncertainty affecting the design of an attitude control system, the entire population of possible wind histories should be considered in an ideal optimization process. A more economical approach is to use synthetic wind profiles representing envelopes of measured winds. The present design scheme makes possible the use of several of these wind profiles simultaneously as a basis for the optimal design.

  If the wind profiles are selected judiciously to represent the most adverse effects on vehicle response, the resulting "trade-off" design will perform satisfactorily not only for the wind extremes used during optimization, but also for all wind conditions of lower magnitude.

- **Optimal Controller Design Insensitive to Parameter Variations.**
  Substantial performance degradation may result if a control system is optimized for nominal operating conditions which differ from the actual conditions due to unpredictable deviations of system parameters from their nominal values. The present optimization method can serve as an efficient new tool to optimize control systems so that they are insensitive to the major parameter variations. The design would be performed in three steps: The upper and lower bounds of all significant system parameters would be estimated and their effects on system performance assessed. Then, several sets of such extreme parameters would be formed which have the most adverse effects upon system response. These adverse operating conditions would then be simultaneously considered during optimization. The resulting design would again represent the best trade-off in view of these most adverse combinations of possible parameter deviations.

To facilitate the use of this new versatile optimization tool, a User's Manual has been prepared (LMSC/HREC D162122-III) which describes the program and its implementation on the hybrid computer.

Section 5
REFERENCES

1. Trautwein, W. , and J. G. Tuck, "Control System Optimization for
    Saturn V Launch Vehicles Using Gradient Techniques," LMSC/HREC
    A791836, Lockheed Missiles & Space Company, Huntsville, Ala.,
    October 1968.

2. Coyne, G. W., and W. Trautwein, "Control System Optimization for
    Saturn V Launch Vehicles Using Gradient Techniques," LMSC/HREC
    D148931, Lockheed Missiles & Space Company, Huntsville, Ala.,
    April 1969.

3. Fletcher, R., and M. J. D. Powell, "A Rapidly Convergent Descent
    Method for Minimization," Computer J., Vol. 6, 1963.

4. Edinger, L. D., et al, "Data Base Report for Saturn V/Voyager Load
    Relief Study," Honeywell Inc. Doc. 21181/SR1, 30 January 1968.

5. MSFC Memo R-AERO-Y-73-65, "Wind Statistics for Preliminary
    Load Studies. . . , " 13 December 1965.

6. MSFC Memo R-AERO-Y-66-65, "Redefinition of Saturn IB/V Synthetic
    Wind Profile, " 10 September 1965.

7. NASA TM X-53023, "Terrestrial Environment Criteria. . . ,"
    13 March 1964.